Catabolism of Adenine Nucleotides and Its Relation with Intracellular Phosphorylated Metabolite Concentration during Ethanol Oxidation in Perfused Rat Liver†

Serge Masson, Franck Desmoulin, Martine Sciaky, and Patrick J. Cozzone*

Centre de Résonance Magnétique Biologique et Médicale, Centre National de la Recherche Scientifique, Unité de Recherche Associée 1186, Faculté de Médecine de la Timone, 27 Boulevard Jean Moulin, 13005 Marseille, France

Received July 31, 1992; Revised Manuscript Received November 9, 1992

ABSTRACT: Ethanol-induced perturbations in the energy metabolism and in the catabolism of adenine nucleotides were investigated by ^{31}P NMR spectroscopy and HPLC analyses in perfused rat liver. Ethanol oxidation reduced the redox potential of the hepatocyte, leading to an intracellular accumulation of *sn*-glycerol 3-phosphate. This accumulation, in turn, led to a cytosolic P_i depletion with a stoichiometric relationship close to 1/1 for an initial period of 2 min. The concentration of nucleoside 5′-triphosphates (83 ± 4% of ATP) was decreased during ethanol oxidation, reaching about 66% of its control value [2.88 ± 0.02 μmol·(g of liver wet wt)$^{-1}$] at high ethanol doses (10 and 70 mM). The depletion of P_i relieved the inhibition exerted by this compound on AMP deaminase, key enzyme in the catabolism of adenine nucleotides. The degradation of AMP was monitored by HPLC analyses of the adenine nucleosides and bases released in the effluents. Integration over time of the total release of these metabolites accounted for the depletion of ATP recorded in the same time by ^{31}P NMR spectroscopy. This result suggests that ATP depletion occurring during ethanol oxidation originated from an enhanced degradation of adenine nucleotides. There was a strong linear correlation ($r^2 = 0.92$) between cytosolic P_i level and allantoin release rate during ethanol perfusion. Cytosolic P_i and allantoin release exhibited biphasic behavior, the recovery toward the initial levels being related to the release of P_i in the cytoplasm during the complete catabolism of adenine nucleotides. Finally, the depletion of P_i affected the glycogenolysis pathway, with a maximal inhibition of ca. 19% of the initial level.

The liver plays a crucial role in the elimination of ethanol in mammals. Two successive oxidations of ethanol by the isoenzymes of alcohol and aldehyde dehydrogenases induce a reduction in the redox potentials of the nicotinamide adenine dinucleotides, both in the cytoplasm and in the mitochondria of hepatocytes (Rawat, 1968). In that way, acute ethanol administration affects numerous metabolic pathways in the liver (Forsander, 1970). Moreover, a chronic and abusive consumption of alcoholic beverages coincides with the emergence of severe hepatic pathologies like alcoholic steatosis, hepatitis, fibrosis, and cirrhosis (Lieber, 1991).

NMR spectroscopy allows the investigation of short-term acute repercussions of ethanol oxidation on liver metabolism as well as the long-term incidences of alcoholism, both on animal models (Helzberg et al., 1987; Takahashi et al., 1990; Brauer & Ling, 1991) and during human clinical studies (Meyerhoff et al., 1989; Angus et al., 1990). The energy metabolism of rat liver has been monitored in vivo after acute administration of ethanol (Cunningham et al., 1986; Quistorff et al., 1987). We have previously documented the ethanol-induced perturbations in the metabolism of perfused rat liver using ^{31}P NMR spectroscopy. Acute perfusion of a high dose of ethanol (70 mM) in livers from fed rats led to an accumulation of *sn*-glycerol 3-phosphate together with a decrease in the amount of ATP and cytosolic P_i (Desmoulin et al., 1987a). The deleterious consequences of ethanol oxidation superimposed to intervals of ischemia have also been investigated (Desmoulin et al., 1987b). Finally, combining HPLC analyses and ^{31}P NMR spectroscopy, we have previously assessed the ethanol-induced inhibition of glycolysis in the perfused rat liver (Masson et al., 1992).

Ethanol consumption is associated with hyperuricemia and by disposition with gout in humans (Grunst et al., 1977; Faller & Fox, 1982; Puig & Fox, 1984). It has been suggested that the decrease in hepatic P_i content, related to *sn*-glycerol 3-phosphate accumulation, could enhance adenine nucleotide catabolism (via a deinhibition of AMP deaminase), similarly to fructose-induced hyperuricemia (Mäenpää et al., 1968; Brosnan et al., 1991). P_i is involved in the regulation of several metabolic pathways (Sestoft & Bartels, 1981). Its cytosolic concentration has been reported to control the step of phosphorolysis during glycogen breakdown in the perfused liver (Vanstapel et al., 1990). P_i has also been involved in the control over oxidative phosphorylation during a metabolic load (Tanaka et al., 1989). In the present study, we have investigated the dose-dependent effect of ethanol on the hepatic content of phosphorylated compounds and stressed the consequences of inorganic phosphate depletion on adenine nucleotide catabolism and glycogenolysis.

EXPERIMENTAL PROCEDURES

Materials. 4-Methylpyrazole and methylenediphosphonic acid were purchased from Sigma Chemical Co. (St. Louis, MO). Ethanol was a HPLC-grade reagent (SDS, Peypin, France).

Liver Perfusion. Male Wistar rats, weighing 240–280 g, were fasted for 24 h and thereafter given a regular chow meal 12 h prior to the experiments. They had free access to water. This protocol enabled us to achieve a high and reproducible level of hepatic glycogen, amounting to 8.3 ± 0.3% (w/w) of

† This work was supported by grants from Centre National de la Recherche Scientifique (URA 1186) and the Institut de Recherches Scientifiques sur les Boissons (Grant 90/03).

* To whom correspondence should be addressed.

0006-2960/93/0432-1025$04.00/0

the liver ($n = 6$) at the beginning of the experiments (Masson et al., 1992). The animals were anesthetized by intraperitoneal injection of sodium pentobarbital (60 mg/kg of body weight). The excised livers (13.43 ± 0.06 g, $n = 36$) were perfused anterogradely in a nonrecirculating mode (Desmoulin et al., 1987a). The perfusion medium consisted of a Krebs–Henseleit solution (Krebs & Henseleit, 1932) with 1.2 mM KH_2PO_4, perfused at a constant rate of 2.8 mL·min^{-1}·(g of liver wet wt)$^{-1}$. The perfusate was oxygenated in a gas exchanger with O_2/CO_2 (19:1) through a silastic tubing (Hamilton et al., 1974), achieving a pH of 7.45. Temperature of the medium was kept constant at 37 °C, up to the liver. After an initial equilibration period (30 min), the perfusion medium was supplemented for 20 min with ethanol, in concentrations ranging from 0.5 to 70 mM. The effluents were continuously collected from the NMR tube with a high-flow peristaltic pump, and sampled every 4 min (for 6 s) to perform HPLC analyses. At the end of this period, the livers were rapidly freeze-clamped between aluminium tongs precooled in liquid nitrogen and then stored at −80 °C. Metabolites were extracted by 7% (v/v) perchloric acid as previously described (Desmoulin et al., 1987a).

^{31}P NMR Spectroscopy. Spectra were obtained using a Bruker WP 200 spectrometer equipped with a superconducting 4.7-T magnet (Bruker, Karlsruhe, Germany). ^{31}P NMR spectra were acquired at 80.9 MHz, without proton decoupling. Perfused livers were set in a 30-mm-diameter NMR tube. Spectra were recorded in blocks of 280 scans by using a nutation angle of 45°, a spectral width of 3600 Hz, and a repetition time of 0.43 s. The total time of acquisition was 2 min. Free induction decays (fid) were processed with an exponential filter corresponding to a 30-Hz line broadening. Moreover, in order to eliminate the broad signal arising mainly from membrane phospholipids, which hampers an accurate quantification (in the phosphomonoesters–phosphodiesters region), a convolution difference with two single-exponential filters, corresponding to a 30- and a 300-Hz line broadening, was applied to the fid's before Fourier transformation. Methylenediphosphonic acid (50 μmol in a sealed glass capillary) was used as an external quantitation standard. Chemical shifts are expressed relative to an 85% H_3PO_4 (w/v) solution at 0.0 ppm. Due to a partial saturation of signal under our regular experimental conditions, areas of resonances were corrected by a saturation factor calculated from spectra recorded under fully relaxed conditions (delay between pulses, 7 s). Concentrations were expressed as micromoles per gram of liver (wet weight).

The ratio between the wet and dry mass of livers amounted to 4.19 ± 0.11 (ratio between the wet mass of an excised lobe blotted on filter paper and the dry mass measured after 48 h of desiccation at 70 °C, $n = 24$). Concentrations of phosphorylated compounds in the cytosol were derived from this ratio and assuming a value of 2.0 mL/g of dry weight for cytosolic water space (Williamson, 1969a).

HPLC Analyses. The HPLC analytical system consisted of a pump, a variable-wavelength UV detector, and a refractive index detector (LKB, Bromma, Sweden). Glucose, lactate, pyruvate, uric acid, and allantoin were assayed in the effluents according to a procedure previously described (Masson et al., 1991), using a strong cation-exchange resin (Aminex HPX 87H, 300 mm × 7.8 mm, Bio-Rad, France), elution with 1.25 mM H_2SO_4 at a constant rate of 0.60 mL·min^{-1}, and a double detection method based on refractometry and UV absorbance at 210 nm. Nucleosides and bases, originating from adenine nucleotide breakdown, were analyzed in the effluents by reverse-phase HPLC using an octadecylsilane stationary-phase column (Lichrospher ODS2 5 m, 250 mm × 4.1 mm, Merck, Darmstadt, Germany). The mobile phase [3% (v/v) acetonitrile in deionized water] was delivered at a rate of 0.8 mL·min^{-1}. The UV detector was set at λ = 254 nm. This rapid isocratic elution (30 min) did not allow an efficient separation of hypoxanthine and xanthine.

Intracellular concentrations of nucleotides in the perchloric acid extracts of the livers were determined by reverse-phase ion-paired chromatography using a C_{18} column (Ultropac TSK ODS 120T, 5 μm, 250 × 4.6 mm, LKB, Bromma, Sweden). The mobile phase [0.2 M NaH_2PO_4, 25 mM tetrabutylammonium, and 6% (v/v) methanol] was delivered at a rate of 1.1 mL·min^{-1}. The ultraviolet detector was set at 254 nm.

All chromatograms were recorded and integrated with dedicated data acquisition and processing software (Kontron Instruments, Munich, Germany). Metabolic rates were calculated from the difference between influent and effluent concentrations, the perfusion rate, and the liver weight and expressed as nanomoles per minute per gram of liver (wet weight). Computing of the release of adenine nucleosides and bases over time was performed by combining the digitization of data (Schlumberger Graphics, France) with integration using dedicated software (AutoCad, Autodesk AG, Switzerland).

Statistics. Data are presented as means ± SEM, with the number of observations in parentheses. The significance of the linear regression was tested using t-statistics.

RESULTS

Effects of Ethanol Concentration on sn-Glycerol 3-Phosphate, P_i, and NTP Levels. A typical ^{31}P NMR spectrum of a perfused rat liver, recorded after a 30 min control period is presented in Figure 1a. Peak assignments have previously been reported (Desmoulin et al., 1987a) and are given in the legend. Figure 1b displays the significant alterations in the spectrum of the same liver after an additional 20-min period of perfusion with a medium supplemented with 10 mM ethanol. There is a large increase in the area of a resonance centered at 4.65 ± 0.02 ppm ($n = 20$), in the phosphomonoesters (PME) peak. We have previously shown that this resonance arises from *sn*-glycerol 3-phosphate (Desmoulin et al., 1987a,b) and that ethanol administration induced a dose-dependent accumulation of G3P, fully detected by ^{31}P NMR spectroscopy (Masson et al., 1992). Initial rates of G3P accumulations, interpolated from data obtained after 2 min of ethanol perfusion, are reported in Table I.

In addition, administration of ethanol induced a depletion in the level of P_i and nucleoside 5′-triphosphates (NTP) (Figure 1b). The kinetic variations of P_i and NTP were monitored with a resolution of 2 min for ethanol concentrations ranging from 0.5 to 70 mM and are presented in Figure 2. The severity of the alterations on P_i and NTP levels was related to ethanol concentration. Trapping of P_i in the form of G3P induced a rapid modification of the cytosolic P_i content as illustrated in Figure 2a. P_i depletion developed for ca. 6 min until a minimum cytosolic P_i level was reached. The control value of P_i content was 1.55 ± 0.01 μmol·(g of liver wet wt)$^{-1}$ ($n = 51$). After 6 min of ethanol perfusion, the levels of cytosolic P_i were decreased to 1.22 ± 0.07 μmol·(g of liver wet wt)$^{-1}$ ($n = 8$) and 0.71 ± 0.05 μmol·(g of liver wet wt)$^{-1}$ ($n = 8$) for ethanol concentrations of 0.5 and 70 mM, respectively. Then, a slow replenishment of cytosolic P_i content occurred. After 20 min of ethanol administration, a complete recovery was observed for 0.5 mM ethanol, whereas only partial

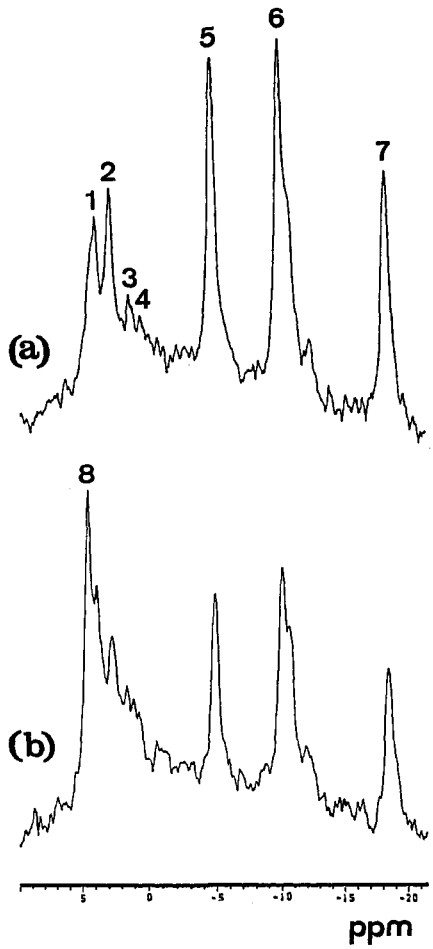

FIGURE 1: ^{31}P NMR spectra of a perfused rat liver. The liver from a fed rat was perfused and NMR spectra were acquired as described in the Experimental Procedures section. Trace a corresponds to a control spectrum and was recorded 30 min after the onset of a Krebs–Henseleit medium perfusion. Spectrum b shows the alterations subsequent to a 20-min perfusion with a medium supplemented with 10 mM ethanol. Assignments of resonances: 1 = phosphomonoesters (mainly phosphorylcholine and AMP); 2 = inorganic phosphate (P_i); 3 = glycero-3-phosphoethanolamine; 4 = glycerol-3-phosphocholine; 5 = γ-phosphorus of NTP and β-phosphorus of NDP; 6 = α-phosphorus of NTP, α-phosphorus of NDP, and NAD^+; 7 = β-phosphorus of NTP; 8 = *sn*-glycerol 3-phosphate.

recoveries were measured at higher ethanol concentrations. Initial rates of P_i depletion, interpolated from data obtained after 2 min of ethanol perfusion, are reported in Table I.

The time-dependent variations of NTP content during ethanol perfusion are presented in Figure 2b. The control value of NTP content determined by ^{31}P NMR spectroscopy was 2.88 ± 0.02 μmol·(g of liver wet wt)$^{-1}$ (n = 51). Analysis of the different nucleoside 5′-triphosphates making up the NTP pool has been performed by HPLC on liver extracts (see Experimental Procedures). In the control liver, the main nucleoside 5′-triphosphate was ATP, accounting for 83 ± 4% of the NTP, with GTP and UTP making up 12 ± 2% and 5 ± 1% (n = 5), respectively. Ethanol oxidation induced a moderate depletion of the NTP content (Figure 2b). For instance, NTP content decreased by ca. 30% after 20 min of ethanol perfusion at 10 or 70 mM. The losses in NTP content measured after 20 min of ethanol perfusion are reported in Table I. Changes in P_i and G3P levels preceded the decrease in NTP level since there were no significant decreases in NTP 2 min after the onset of ethanol perfusion.

Although the quantification of hepatic NDP by NMR is not perfect in livers from normal rats, a free NDP level could be estimated by subtracting the area under the resonance of β-phosphate of NTP from the resonance arising from both the γ-phosphate of NTP and the β-phosphate group of NDP. Any detectable modifications of the NDP content were observed during ethanol perfusions from 0.5 to 70 mM (data not shown).

In the presence of 1 mM 4-methylpyrazole, a potent inhibitor of alcohol dehydrogenase, G3P, NTP, and P_i contents were not altered after the perfusion of 10 mM ethanol to livers (n = 3, data not shown).

Catabolism of Adenine Nucleotides during Ethanol Oxidation. In order to document whether the ethanol-induced depletion of NTP could be explained by an increase in the degradation of adenine nucleotides, similarly to the mechanism occurring during fructose-induced hyperuricemia (Mäenpää et al., 1968), the release of adenine nucleotide catabolites in the liver effluents has been monitored. The adenine nucleosides and bases were analyzed by HPLC as described in the Experimental Procedures section. The time course of the release of inosine, hypoxanthine, xanthine, uric acid, and allantoin was determined for perfusions of ethanol at a concentration of 10 mM. During control experiments, the cumulative output of adenine nucleotide catabolites amounted to 10.90 ± 1.80 nmol·min^{-1}·(g of liver wet wt)$^{-1}$ (n = 5) and remained constant throughout the experiments. The main product was uric acid, representing 65 ± 5% of the catabolite pool, when allantoin and the (inosine + hypoxanthine + xanthine) sum made up 21 ± 3% and 14 ± 2%, respectively (n = 5). On the other hand, following the administration of 10 mM ethanol, the release of adenine nucleotide breakdown products increased and reached a maximum after 8 min (Figure 3). Most notably, the release of allantoin increased from a control value of 3.01 ± 0.16 to 27.20 ± 3.88 nmol·min^{-1}·(g of liver wet wt)$^{-1}$ (n = 16). Thereafter, the release of the products decreased. It is noteworthy that the release of adenosine never exceeded 0.12 nmol·min^{-1}·(g of liver wet wt)$^{-1}$ during either control experiments or ethanol perfusions.

The output of adenine nucleotide catabolites in the effluents has been integrated over the duration of experiments (20 min). The loss of adenine nucleotides amounted to 218 ± 56 nmol·(g of liver wet wt)$^{-1}$ (n = 5) after 20 min for the control experiments and 868 ± 105 nmol·(g of liver wet wt)$^{-1}$ (n = 16) in the meantime during ethanol oxidation (10 mM). Almost 44% of the latter loss was imputable to the release of allantoin. The losses should be compared with the depletion of NTP detected by ^{31}P NMR after 20 min of experiment, reported in Table I.

Figure 4 displays the time-dependent dose effect of ethanol perfusion on the allantoin release. A 9-fold increase in allantoin release rate was observed at 10 and 70 mM ethanol versus control (no ethanol), 8 min after alcohol administration. In the presence of 1 mM 4-methylpyrazole and 10 mM ethanol, allantoin release rate was not affected throughout the experiments (n = 3).

DISCUSSION

Ethanol indirectly exerts a P_i-depleting action because, similar to fructose (Woods et al., 1970), xylulose (Vincent et al., 1989), and glycerol (Sestoft & Fleron, 1975), it provokes the accumulation of a phosphate ester (*sn*-glycerol 3-phosphate) inside the hepatocyte (Figure 1b). In this work, accumulation of G3P is due to the increase in the NADH/NAD^+ ratio during ethanol oxidation (Rawat, 1968). A direct action of ethanol can be ruled out since it has no incidence

Table I: Metabolic Rates and NTP Depletion in Perfused Rat Liver following Ethanol Administration[a]

	[ethanol] (mM)					
	70 (n = 8)	10 (n = 16)	2.0 (n = 10)	1.0 (n = 9)	0.5 (n = 8)	0 (n = 3)
initial rate of G3P accumulation [μmol min^{-1} (g wet wt of liver)$^{-1}$]	0.35 ± 0.05	0.34 ± 0.03	0.26 ± 0.05	0.17 ± 0.04	0.11 ± 0.04	*b*
inital rate of P_i depletion [μmol min^{-1} (g wet wt of liver)$^{-1}$]	0.31 ± 0.04	0.30 ± 0.06	0.23 ± 0.07	0.13 ± 0.06	0.10 ± 0.06	*b*
NTP depletion[c] (NMR) [μmol (g wet wt of liver)$^{-1}$]	0.96 ± 0.03	0.95 ± 0.09	0.75 ± 0.07	0.46 ± 0.06	0.23 ± 0.05	0.18 ± 0.04

[a] The initial rates of *sn*-glycerol 3-phosphate accumulation and P_i depletion are calculated from ^{31}P NMR data obtained 2 min following ethanol administration. The NTP depletion is determined by the difference between control NTP level (2.88 ± 0.02 μmol/g of liver wet wt) and NTP level at the end of experiments, after 20 min of ethanol administration. Data are expressed as means ± SEM. [b] Not measurable; the resonances corresponding to G3P and P_i remain in the noise of the difference spectra. [c] The control value of NTP was 2.88 ± 0.02 μmol (g wet wt of liver)$^{-1}$ (n = 51).

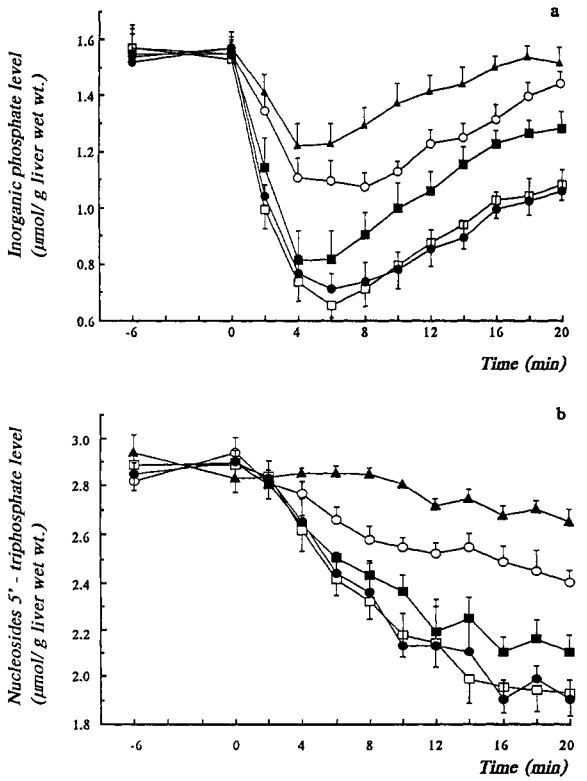

FIGURE 2: Time course and dose-dependent effects of ethanol perfusion on intracellular P_i and NTP levels. Livers were first perfused with a Krebs–Henseleit buffer for 30 min. At the zero time point, various amounts of ethanol were added to the perfusate. Spectra were recorded every 2 min. Evolutions of inorganic phosphate (a) and nucleoside 5'-triphosphates (b) are presented for ethanol concentrations of 0.5 mM (▲), 1.0 mM (○), 2.0 mM (■), 10 mM (□), or 70 mM (●). Values shown are means ±SEM for the number of experiments reported in Table I. For the sake of clarity, only half of the vertical bars are drawn.

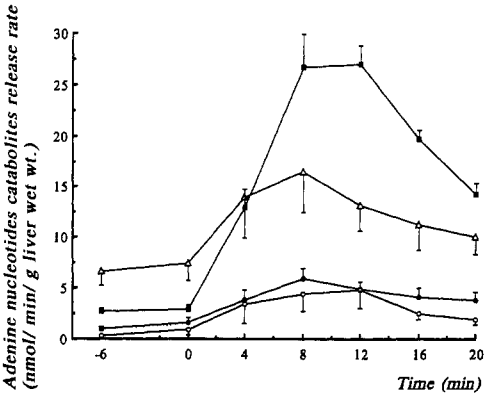

FIGURE 3: Time course of adenine nucleotide catabolites release during ethanol oxidation. Livers were first perfused with a Krebs–Henseleit buffer for 30 min. At the zero time point, 10 mM ethanol was added to the perfusate. The effluent medium was sampled every 4 min to perform HPLC analyses of the adenine nucleotide catabolism products as described in Experimental Procedures. The output of uric acid (△), allantoin (■), xanthine + hypoxanthine (●), and inosine (○) are displayed. Data are presented as means ±SEM for either 16 experiments (allantoin) or 5 experiments (uric acid, inosine, and hypoxanthine + xanthine). For the sake of clarity, only half of the vertical bars are drawn.

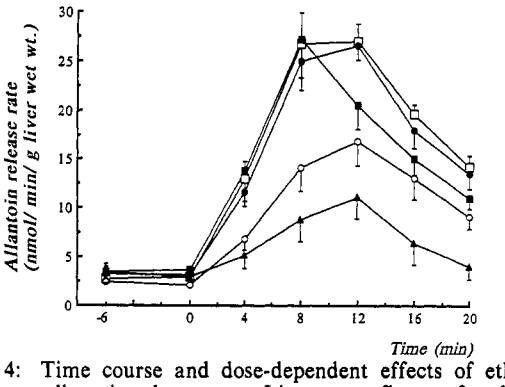

FIGURE 4: Time course and dose-dependent effects of ethanol oxidation on allantoin release rate. Livers were first perfused with a Krebs–Henseleit buffer for 30 min. At the zero time point, various amounts of ethanol were added to the perfusate. The effluent was sampled every 4 min to perform HPLC analysis of allantoin during ethanol perfusions at concentrations of 0.5 mM (▲), 1.0 mM (○), 2.0 mM (■), 10 mM (□), or 70 mM (●). Results are presented as means ±SEM for the number of experiments reported in Table I. For the sake of clarity, only half of the vertical bars are drawn.

on ^{31}P NMR spectra and adenine nucleotide breakdown products release in presence of 4-methylpyrazole, a potent inhibitor of alcohol dehydrogenase. Ethanol oxidation induces a dose-dependent accumulation of G3P up to a concentration of 10 mM. Large accumulation of G3P during ethanol administration occurs in the liver from fed rats, where glycogen content is high, but not in the livers from fasted rats in the absence of glycolytic substrates. In the early phase of ethanol administration (until 2 min), the cytosolic P_i depletion appears to be quantitatively related to G3P accumulation, with a stoichiometric relationship close to 1/1 (Table I). We have previously shown that, under the same experimental conditions, ethanol oxidation induced only a slight increase in the liver oxygen consumption, from a basal value of 1.80 ± 0.05 to 1.85 ± 0.06 μmol of O_2·min^{-1}·(g of liver wet wt)$^{-1}$, not dependent upon ethanol concentration between 0.5–1.0 and 70 mM (Masson et al., 1992). Assuming a P/O ratio of 3, the basal ATP synthesis rate is then 10.8 μmol·min^{-1}·(g of liver wet wt)$^{-1}$. This rate is only slightly increased to 11.1 μmol·min^{-1}·(g of liver wet wt)$^{-1}$ at the onset of ethanol oxidation. When glycogen is the main substrate, the formation of 2 mol of G3P requires 1 mol of P_i and 1 mol of ATP. A maximal rate of 0.35 μmol·min^{-1}·(g of liver wet wt)$^{-1}$ for G3P accumulation has been measured at 10 or 70 mM ethanol concentrations, corresponding to an initial rate of ATP consumption of 0.17 μmol·min^{-1}·(g of liver wet wt)$^{-1}$. Therefore, the ATP consumption rate imputable to G3P accumu-

lation represents only 1.5% of the overall ATP production rate. This could explain why ATP content remains constant during an initial period of 2 min (Figure 2b) and why we have not measured any increase in the liver ADP content. In contrast, during fructose administration, the accumulation of phosphomonoester is much faster, being 12 μmol·min^{-1}·(g of liver wet wt)$^{-1}$ for fructose 1-phosphate (Van den Berghe et al., 1977). In that case, ADP production rate overruns ATP synthesis rate. A transient increase in ADP content concomitant with a swift decrease in ATP level has actually been observed during the fructose ester accumulation (Mäenpää et al., 1968; Van den Berghe et al., 1977). Nevertheless, the 2–3-fold increase in ADP elicited by fructose administration in livers from control or transgenic mice (expressing creatine kinase *b*) was not sufficient to account for the depletion of ATP (Brosnan et al., 1991).

During the next 18 min of ethanol administration, the hepatic content of NTP decreases significantly, down to 66% of its initial value for the highest concentration of ethanol (Figure 2b). This depletion contrasts with the stability of ATP observed after ethanol administration in livers from fasted rats in vivo (Veech et al., 1972; Cunningham et al., 1986) or perfused (Williamson et al., 1969b; Desmoulin et al., 1987a) but is in agreement with a previous study conducted with perfused livers from rats fed ad libitum (Desmoulin et al., 1987a). This decrease cannot be related to a limitation of oxidative phosphorylation or to an increase in the ATP consumption rate since the oxygen consumption (Masson et al., 1992) and the NDP level remain constant during the experiment. These observations led us to investigate the regulation of adenine nucleotide catabolism during ethanol oxidation.

Adenine Nucleotide Catabolism Accounts for ATP Depletion. AMP deaminase constitutes the rate-limiting step of the adenine nucleotide catabolism pathway in rat liver. The role of P_i as a potent inhibitor of AMP deaminase is well established (Van den Berghe, 1981). The ethanol-induced accumulation of G3P, by trapping inorganic phosphate, could hence relieve the inhibition exerted by P_i on AMP deaminase and then increase the catabolism of adenine nucleotides. Moreover, since ATP, ADP, and AMP are maintained at equilibrium by the adenylate kinase (Veech et al., 1972), the catabolism of adenine nucleotides would affect the whole pool. To test this hypothesis, the compounds arising from adenine nucleotide catabolism and released in the effluents during ethanol oxidation have been analyzed. Before ethanol administration, uric acid is the main base released by the liver (65 ± 5%). During ethanol oxidation, allantoin, the end product of the catabolic pathway in rat liver, becomes the major compound, making up 50% of the adenine nucleotide breakdown products. The intermediary nucleoside and bases (inosine, hypoxanthine, and xanthine) remain at a constant level of ca. 13%, suggesting that the flux through the adenine nucleotide degradation pathway is not limited at their level. Adenosine release rate was always lower than 0.12 nmol·min^{-1}·(g of liver wet wt)$^{-1}$ and remained unaffected by ethanol oxidation. This low value is in good agreement with the results of Arnold and Cysyk (1986), who found a dependency (increase) of adenosine export from the liver when the oxygen tension was lowered in the perfusate. It thereby confirms an adequate O_2 consumption rate for our perfused organs. Moreover, this low release of adenosine is consistent with a first step of AMP catabolism catalyzed by AMP deaminase but not 5′-nucleotidase in rat liver (Van den Berghe et al., 1977). For a concentration of ethanol of 10 mM, the integrated output of adenine nucleotide breakdown products during ethanol oxidation [0.868 μmol·(g of liver wet wt)$^{-1}$], almost matches the ATP loss recorded by ^{31}P NMR spectroscopy [0.95 μmol·(g of liver wet wt)$^{-1}$, Table I]. Adenosine 5′-triphosphate is indeed the major component of liver NTP, making up 83% of NTP under our conditions, in agreement with other reports (Floridi et al., 1977; Palombo et al., 1988). Therefore, one may conclude that NTP content is decreased during ethanol oxidation as a result of a complete catabolism of adenine nucleotides.

Biphasic Behavior of Cytosolic Inorganic Phosphate. P_i level evolution is not monotonous over the duration of the experiment. Indeed, after the P_i level has reached a minimal value after 6 min of ethanol perfusion, an increase in P_i content is measured until the end of the experiment. In agreement with this observation, Vincent et al. (1989) have described a similar biphasic behavior for P_i after xylitol administration to hepatocytes. They related P_i recovery to the restoration of pentose phosphate levels, which increase during xylitol oxidation, before entering the gluconeogenic pathway above the glyceraldehyde-3-phosphate dehydrogenase level. The conversion of pentose phosphates to glucose was accompanied by a release of P_i. Moreover, the rate of P_i recovery was dependent on the rate of phosphorylation of various ATP-depleting substances, with a slower recovery of intracellular P_i associated with a lower rate of conversion to glucose for xylitol compared with D-xylulose (Vincent et al., 1989), suggesting a limited role for extracellular P_i during this phase of intracellular P_i recovery. Similarly, the catabolism of AMP provokes the release of ribose 1-phosphate by the nucleoside phosphorylase, which produces hypoxanthine and ribose 1-phosphate from inosine. Ribose 1-phosphate can be converted to ribose 5-phosphate by phosphoribomutase, then reaching the pentose phosphate pathway and the gluconeogenic pathway. Glucose is formed and P_i is liberated in the cytosol. As P_i release starts to exceed its consumption by oxidative phosphorylation and its trapping as G3P, the level of cytosolic P_i increases.

Relationship between Allantoin Release Rate and P_i Concentration. The allantoin release curves exhibited a biphasic shape during ethanol oxidation, whatever the concentration of alcohol administered (Figure 4). This shape was inversely related to the behavior of cytosolic P_i detected by ^{31}P NMR under the same conditions (Figure 2a). In fact, there was a strong linear correlation ($r^2 = 0.92$, $p < 0.001$) between the mean values of allantoin release collected during ethanol oxidation for different concentrations of ethanol (from 0.5 to 70 mM) and the corresponding values of cytosolic P_i, as displayed in Figure 5. Kinetic studies on AMP deaminase have revealed the requirement of both GTP and P_i to exert an efficient inhibition on this enzyme (Van den Berghe, 1981). Regarding the concentrations of ATP, GTP, and P_i, expressed as millimolar in the cytosol, and the kinetic behavior of AMP deaminase, some comments about the control of its activity under our conditions may be inferred. Indeed, ethanol administration elicits a maximal decrease in P_i concentration from 3.25 to 1.43 mM. In the same manner, ATP and GTP decrease from 5.01 to 3.51 mM and from 0.72 to 0.51 mM, respectively, assuming that GTP decrease is proportional to ATP decrease. In fact, this assumption overestimates the actual GTP decrease, which has been reported to occur at a slower rate than ATP decrease (Van den Berghe et al., 1977). Kinetic data reported by Van den Berghe et al. (1977) show that GTP concentrations higher than 0.5 mM induce a maximal inhibition on the ATP-activated AMP deaminase.

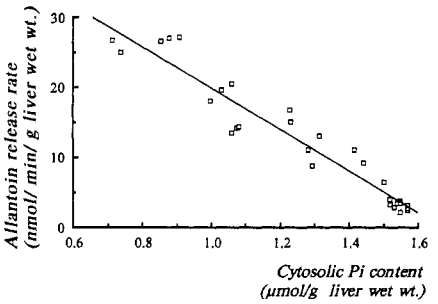

FIGURE 5: Relationship between allantoin release rate and cytosolic P_i level during ethanol administration. Mean values of allantoin release rate in the effluents obtained from HPLC analysis displayed in Figure 4 are plotted against mean values of P_i content determined from ^{31}P NMR spectroscopy from Figure 2a. The average data recorded from 8 min after ethanol oxidation are presented. A regression line calculated from 30 pairs of data follows the equation $y = 49.5 - 29.6x$ ($r^2 = 0.92$, $p < 0.001$).

Since, under our conditions, GTP concentration does not fall below 0.5 mM, it can be assumed that the control of the enzyme is devoted to P_i, therefore explaining the linear correlation observed between allantoin release rate and the cytosolic P_i content. Likewise, evidence that P_i is an important inhibitor of AMP deaminase in vivo and at physiological concentrations in mice livers subjected to fructose loads has been recently reported (Brosnan et al., 1991).

Involvement of P_i in Ethanol-Induced Inhibition of Hepatic Glycogenolysis. The glycogenolytic pathway is mainly regulated through the interconversion of glycogen phosphorylase between its active phosphorylated (*a*) form and its dephosphorylated form (*b*). Glycogenolysis is also modulated by the intracellular level of some effectors, including inorganic phosphate (Van de Werve, 1981). Ethanol administration may therefore affect glycogenolysis by a control over phosphorylase interconversion and/or a lowering of intracellular P_i concentration. This latter regulation has previously been investigated in perfused rat livers where glycogen phosphorylase was fully converted into the *a* form by exposure to dibutyryl-cAMP, and a linear relationship was observed between the rate of glycogenolysis (expressed as the release of hexose equivalents) and cytosolic P_i concentration (Vanstapel et al., 1990). In the present study, the involvement of cytosolic P_i in the regulation exerted on the pathway of glycogenolysis has been assessed during ethanol perfusion to fed rat livers. The sum of the combined releases of glucose, lactate, and pyruvate (as hexose equivalents) in the effluents was assumed to represent an estimate of the glycogen breakdown inside the liver (Thurman & Scholz, 1977; Soboll et al., 1981). Figure 6 shows the comparative time courses of P_i and glycogenolysis during 10 mM ethanol perfusion. In the absence of ethanol, a basal glycogenolysis rate of 1.88 ± 0.07 μmol of hexose equiv·(g of liver wet wt)$^{-1}$·min^{-1} has been measured, and after 4 min of ethanol administration, a significant maximal inhibition of 19.2 ± 1.9% ($n = 6$) has been found. Ethanol has been shown to decrease the specific activity of glycogen phosphorylase in livers from male rats submitted to a chronic alcohol ingestion, though this inhibition was relieved by addition of AMP (Winston & Reitz, 1981). The specific activity of phosphorylase kinase, the enzyme catalyzing the conversion of phosphorylase *b* into the *a* form, was also decreased after ethanol administration in human and rabbit muscles preparations (Cussó et al., 1989). However, under conditions where hepatic glycogen stores are maximal [8.3 ± 0.3% (w/w) of the liver in the present study], the inactivation of phosphorylase is inhibited and the phosphorylase kinase is stimulated (Van de Werve, 1981).

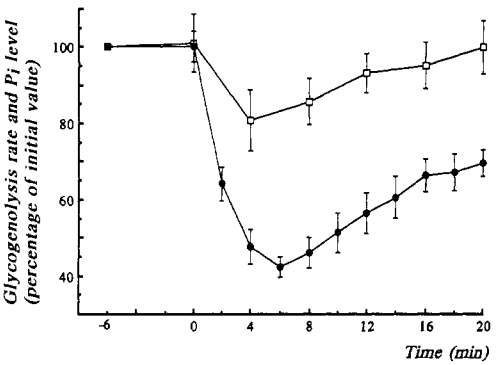

FIGURE 6: Time course of glycogenolysis rate and P_i level during ethanol perfusion. Livers were first perfused with a Krebs–Henseleit buffer for 30 min. At the zero time point, 10 mM ethanol was added to the perfusate. The cytosolic level of P_i (from NMR data) (●) and the rate of release of hexose equivalents (□) are expressed relative to the levels recorded before the addition of ethanol. Glycogenolysis rate was sampled every 4 min. Data are expressed as means ±SEM for 16 experiments for P_i determination and 6 experiments for glycogenolysis rate.

Moreover, the time course variations of glycogenolysis rate paralleled fairly well the P_i level during ethanol oxidation, with biphasic behavior (Figure 6). Thus, although a direct modulation exerted by ethanol on the activation of glycogen phosphorylase cannot be excluded in this study, our results support the involvement of P_i in the regulation of phosphorylase *a* activity in liver cells, in agreement with others (Stermann et al., 1978; Vanstapel et al., 1990).

REFERENCES

Angus, P. W., Dixon, R. M., Rajagopalan, B., Ryley, N. G., Simpson, K. J., Peters, T. J., Jewell, D. P., & Radda, G. K. (1990) *Clin. Sci. 78*, 33–38.

Arnold, S. T., & Cysyk, R. L. (1986) *Am. J. Physiol. 251*, G34–G39.

Brauer, M., & Ling, M. (1991) *Magn. Reson. Med. 20*, 100–112.

Brosnan, M. J., Chen, L., Wheeler, C. E., Van Dyke, T. A., & Koretsky, A. P. (1991) *Am. J. Physiol. 260*, C1191–C1200.

Cunningham, C. C., Malloy, C. R., & Radda, G. K. (1986) *Biochim. Biophys. Acta 885*, 12–22.

Cussó, R., Vernet, M., Cadefeau, J., & Urbano-Marquez, A. (1989) *Alcohol Alcoholism 24*, 291–297.

Desmoulin, F., Cozzone, P. J., & Canioni, P. (1987a) *Eur. J. Biochem. 162*, 151–159.

Desmoulin, F., Canioni, P., Crotte, C., Gérolami, A., & Cozzone, P. J. (1987b) *Hepatology 7*, 315–323.

Faller, J., & Fox, I. H. (1982) *N. Engl. J. Med. 307*, 1598–1602.

Floridi, A., Palmerini, C. A., & Fini, C. (1977) *J. Chromatogr. 138*, 203–212.

Forsander, O. A. (1970) *Q. J. Stud. Alcohol 31*, 550–570.

Grunst, J., Dietze, G., & Wicklmayr, M. (1977) *Nutr. Metab. 21*, 138–141.

Hamilton, R. L., Berry, M. N., Williams, M. C., & Severinghaus, E. M. (1974) *J. Lipid Res. 15*, 182–186.

Helzberg, J. H., Brown, M. S., Smith, D. J., Gore, J. C., & Gordon, E. R. (1987) *Hepatology 7*, 83–88.

Krebs, H. A., & Henseleit, K. (1932) *Hoppe-Seyler's Z. Physiol. Chem. 210*, 33–66.

Lieber, C. S. (1991) *Alcohol: Clin. Exp. Res. 15*, 573–593.

Mäenpää, P. H., Raivio, K. O., & Kekomäki, M. P. (1968) *Science 161*, 1253–1254.

Masson, S., Sciaky, M., Desmoulin, F., Fontanarava, E., & Cozzone, P. J. (1991) *J. Chromatogr. (Biomed. Appl.) 563*, 231–242.

Masson, S., Desmoulin, F., Sciaky, M., & Cozzone, P. J. (1992) *Eur. J. Biochem. 205*, 187–194.

Meyerhoff, D. J., Boska, M. D., Thomas, A. M., & Wiener, M. W. (1989) *Radiology 173*, 393–400.
Palombo, J. D., Hirschberg, Y., Pomposelli, J. J., Blackburn, G. L., Zeisel, S. H., & Bistrian, B. R. (1988) *Gastroenterology 95*, 1043–1055.
Puig, J. G., & Fox, I. H. (1984) *J. Clin. Invest. 74*, 936–941.
Quistorff, B., Pedersen, E. J., McCully, K., & Chance, B. (1987) in *NMR Spectroscopy in Drug Research* (Jaroszewski, J. W., Schaumburg, K., & Kofod, H., Eds.) Alfred Benzon Symposium 26, Munksgaard, Copenhagen, Denmark.
Rawat, A. K. (1968) *Eur. J. Biochem. 6*, 585–596.
Sestoft, L., & Fleron, P. (1975) *Biochim. Biophys. Acta 375*, 462–471.
Sestoft, L., & Bartels, P. D. (1981) in *Short-Term Regulation of Liver Metabolism* (Hue, L., & Van de Werve, G., Eds.) pp 427–452, Elsevier, Amsterdam.
Soboll, S., Heldt, H.-W., & Scholz, R. (1981) *Hoppe-Seyler's Z. Physiol. Chem. 362*, 247–260.
Stermann, R., Wagle, S. R., & Decker, K. (1978) *Eur. J. Biochem. 88*, 79–85.
Takahashi, H., Geoffrion, Y., Butler, K. W., & French, S. W. (1990) *Hepatology 11*, 65–73.
Tanaka, A., Chance, B., & Quistorff, B. (1989) *J. Biol. Chem. 264*, 10034–10040.
Thurman, R. G., & Scholz, R. (1977) *Eur. J. Biochem. 73*, 13–21.
Van den Berghe, G. (1981) in *Short-Term Regulation of Liver Metabolism* (Hue, L., & Van de Werve, G., Eds.) pp 361–376, Elsevier, Amsterdam.
Van den Berghe, G., Bronfman, M., Vanneste, R., & Hers, H.-G. (1977) *Biochem. J. 162*, 601–609.
Vanstapel, F., Waebens, M., Van Hecke, P., Decannière, C., & Stalmans, W. (1990) *Biochem. J. 266*, 207–212.
Veech, R. L., Guynn, R., & Veloso, D. (1972) *Biochem. J. 127*, 387–397.
Vincent, M. F., Van den Berghe, G., & Hers, H.-G. (1989) *FASEB J. 3*, 1855–1861.
Williamson, J. R. (1969a) in *The Energy Level and Metabolic Control in Mitochondria* (Papa, S., Tager, J. M., Quagliarello, E., & Slater, E. C., Eds.) pp 385–400, Adriatica Editrice, Bari, Italy.
Williamson, J. R., Scholz, R., Browning, E. T., Thurman, R. G., & Fukami, M. H. (1969b) *J. Biol. Chem. 244*, 5044–5054.
Winston, G. W., & Reitz, R. C. (1981) *Am. J. Clin. Nutr. 34*, 2499–2507.
Woods, H. F., Eggleston, L. V., & Krebs, H. A. (1970) *Biochem. J. 119*, 501–510.